[AMERICAN JOURNAL OF SCIENCE, VOL. 278, OCTOBER, 1978, P. 1085-1098]

ARC LENGTHS OF SINGLE LAYER FOLDS: A DISCUSSION OF THE COMPARISON BETWEEN THEORY AND OBSERVATION

RAYMOND C. FLETCHER* and JO-ANN SHERWIN**

ABSTRACT. Low limb-dip fold train profiles were simulated numerically by Fourier synthesis from known amplitude spectra in order to determine empirical relations between the frequency distributions of fold arc length and the spectra. The mean fold arc length is approximately equal to the wavelength of the component for which the limb-dip is a maximum. If the initial amplitude spectrum that is selectively amplified in the folding process corresponds to uniform initial limb-dip, the mean fold arc length will be approximately equal to the wave length of the component that has received the maximum amplification, in agreement with Sherwin and Chapple (1968).

INTRODUCTION

In the early stages of the folding of a competent layer, the initial irregular waviness in layer shape is selectively amplified into a more or less regular train of low limb-dip folds. During this phase, the layer undergoes nearly uniform thickening. When the limb-dips reach 10° to 20°, a transition between uniform layer thickening and folding at uniform thickness takes place, and the wavelength selection process breaks down. The positions of the hinges of the finite-amplitude folds, measured in arc length along the layer, preserve the positions of the local minima and maxima, or maxima in curvature, in the low limb-dip fold train at the termination of the selection process. This information is lost only when the folds become tightly appressed, and the limbs are extended, and the hinge regions thickened.

Wavelength-selection is the part of the folding process most sensitive to the rheological properties of layer and medium. The theory of wavelength-selection is well established (Biot, 1961; Sherwin and Chapple, 1968; Fletcher, 1974). For these reasons, the interpretation of the characteristic fold arc length/thickness ratio and the degree of regularity in natural fold populations provides a good opportunity to obtain information on rheological properties of rock during slow tectonic deformation. Of particular interest are applications in situations where the effective viscosity of one rock can be obtained relative to a material whose rheological behavior is well understood from experimental studies — for example, the matrix of a folded quartz vein; and in situations where the rheological behavior is not easily amenable to experimental study — for example, when the deformation involves mass transport of a soluble phase.

Since Sherwin and Chapple's (1968) initial work on interpreting natural populations of single-layer folds on the basis of wavelength-selection theory, no refinements to the method have been made. Several questions about the interpretation can be raised, however, and the possibility of some refinement exists.

* Geology Department, School of Earth Sciences, Stanford University, Stanford, California 94305

* IMEC, Inc., P.O. Box 426, Inez, Kentucky 41224

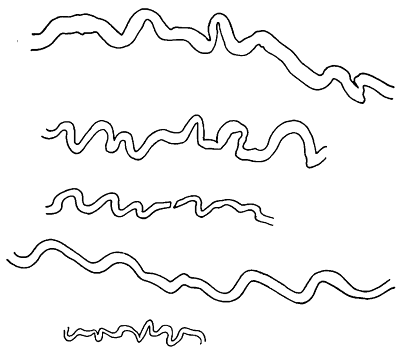

Fig. 1. Segments of folded quartz veins embedded in phyllite.

First, we may ask what precisely is observed in a fold train? Earlier work (Currie, Patnode, and Trump, 1962), in which folds were interpreted as arising from elastic buckling in which a distinct mode of instability arises (see their experimental results), perhaps suggested the notion of a "fold wavelength." Biot (1961) supposed that if folds in layered viscous media were to occur at all, conditions must correspond to the existence of a relatively strong folding instability. He suggested that the maximum amplification would typically be greater than 1000, corresponding to a relatively narrow range of wavelength over which components in the layer shape have appreciable amplitude. This again suggests a highly regular, quasi-periodic fold train. In fact, natural fold trains generally show a substantial degree of irregularity. This is especially clear when one collects a large population for an interpretative study, rather than photographs the most striking example in a series of outcrops. Examples from the largest collection studied in Sherwin and Chapple (1968) are shown in figure 1. It is not easy to imagine here that one is directly observing a "fold wavelength." Although one may wish to use the mean fold arc length[1] as an estimate for the wavelength that has received the maximum amplification, it is not necessary to think of it as a wavelength.

On the other hand, the nature of the profile of a low limb-dip fold train is well understood. Consider an initial layer shape resolved into its Fourier components. In the folding process, these components are independently and selectively amplified, resulting in an amplification spectrum with a maximum near the wavelength of the component that has received the maximum amplification. The superposition of components, with initial random phase, results in a more or less smooth and regular, but nonperiodic, fold train profile. The profile will be smooth at a length scale equal to the layer thickness. The positions of the incipient fold hinges, or local maxima in curvature, cannot be interpreted in any more definite way than as the outcome of the superposition of components with random phase. Hence, the distances between them should

[1] Hereafter we shall suppose that wavelengths or fold arc lengths are measured in units of the layer thickness.

not be interpreted as wavelengths. Wavelength implies periodicity as well as regularity. Moreover, there is apparently no direct mathematical operation that would permit us to derive the frequency distribution of arc lengths between successive hinges from the given amplitude spectrum (William Hrushka, personal commun.). This suggests that it may be worthwhile to reexamine Sherwin and Chapple's (1968) assumption that the mean fold arc length is a good estimate for the wavelength of the component that has received the maximum amplification. One purpose of the present work is to test this assumption and modify it if necessary. In the first part of the paper, we establish empirical relations between the properties of low limb-dip amplitude spectra and those of the corresponding frequency distributions of fold arc length. We synthesize low limb-dip fold train profiles from a given amplitude spectrum. The frequency distribution of fold arc length is extracted from the synthesized fold trains. This is repeated for a set of amplitude spectra that have different relative bandwidths. We find that:

1. the mean fold arc length is approximately equal to the wavelength of the component with the maximum *limb-dip,* irrespective of the relative bandwidth of the spectrum; and
2. the degree of regularity in fold arc length, which can be measured by the dispersion (standard deviation/mean) of the frequency distribution, varies smoothly with the relative bandwidth of the amplitude spectrum.

These empirical relations can be used to estimate two properties of the low limb-dip amplitude spectrum — the relative bandwidth and the wavelength of the component whose limb-dip is maximum — from two properties of the observed frequency distribution of fold arc length — the mean and the dispersion.

To link observation, which provides estimates of properties of the low limb-dip amplitude spectrum, and theory, which provides model amplitude spectra, we need to determine or estimate an initial amplitude spectrum. (Amplitude equals initial amplitude times amplification.) In the absence of data on the initial shapes of folded layers, we choose an initial amplitude spectrum corresponding to uniform initial limb-dip. It can then be shown that the component in the final amplitude spectrum with the maximum limb-dip is also the component that has received the maximum amplification. Together with the result (1), this confirms Sherwin and Chapple's (1968) assumption.

SIMULATION OF FOLD TRAINS

The fold train profile.—Available folding theory cannot deal with non-cylindrical folds, and we consider only the folding of a layer whose shape is cylindrical. We can think of the fold train profile as a single curve corresponding either to the mid-line of the layer cross section or to the average of its upper and lower surfaces. Irregularities in the profile at a scale smaller than the layer thickness are not important in the folding process and can be ignored. The fold train profile will, therefore, be imagined to be smooth below a scale of about 1/10 the typical fold arc length, corresponding to natural folds with typical fold arc length/ thickness ratios of ten or less.

During the early stage of folding, the layer takes on the more-or-less regular shape that we associate with a fold train. Given an initial layer shape, the folding theory applicable at low limb-dip permits us to follow the evolution of the layer shape to the point where the selection process breaks down. We consider fold train profiles established at this point.

The model amplitude spectra.—In principle, it would be possible to generate a low limb-dip amplitude spectrum from a theoretically derived amplification spectrum and a given initial amplitude spectrum. We by-pass this procedure and use amplitude spectra of simple analytical form. We were concerned with the adequacy of our simulation procedures and wished to deal with spectra with an uniform form but different relative bandwidths. The results of the simulation are not likely to depend strongly on the details of the spectrum shape. The present *amplitude* spectra are skewed toward longer wavelength as is typical of theoretical *amplification* spectra (Sherwin and Chapple, 1968; Fletcher, 1974).

The amplitude spectra used have the form

$$A(k) = \exp\,[(ln\,k/ln\,k')^2 ln\,(0.5)], \tag{1}$$

where k is wavenumber, and k′ is a wavenumber related to the relative bandwidth. Spectrum (1) has the symmetry property

$$A(1/k) = A(k); \tag{2}$$

it is skewed toward smaller values of k and also smaller values of wavelength, $L = 2\pi/k$. Since we are not concerned with the absolute amplitude, nor with the absolute values of wavelengths, (1) is a normalized spectrum with maximum amplitude 1 at wavelength $L_p = 2\pi$ or wavenumber $k_p = 1$. From (1)

$$A(k') = A(1/k') = 0.5 \tag{3}$$

so that the relative bandwidth of the spectrum (Biot, 1961), taking $k' < 1$, is

$$\beta = (1/k'-k')/k_p = 1/k'-k'. \tag{4}$$

Simulation procedure.—Fold train segments of arbitrary length 100π, or fifty times wavelength L_p, were generated as a set of discrete coordinates (x_j, z_j) equally spaced in the horizontal coordinate x, using the finite Fourier series

$$z(x) = \sum_{n=1}^{N} A_n(k_n)\cos(k_n x + \phi_n) \tag{5}$$

The ϕ_n are a random set of phase angles drawn from a population that is uniformly distributed in the interval $(0, 2\pi)$. This choice implies an initial irregularity that is uniformly distributed in amplitude along the layer, rather than local bumps spaced at a scale much greater than the preferred wavelength (see Biot, Odé, and Roever, 1961; Cobbold, 1975). (The present model does not apply to the case of folding that "propagates" from such large localized irregularities. This aspect has not been investigated.) The k_n were chosen to be spaced equally in ln k, and the N values chosen were equally partitioned on either side of value k_p. Thus, the wavelengths do not have an harmonic relationship to each other as they would if k_n were equally spaced in k. This means that no periodicity will be presented in a fold train segment of length S, even though the largest wavelength used is significantly less than S. If L_p is supposed to be about ten times the layer thickness, which seems to be appropriate for many natural single-layer folds, the restriction $k_n \lesssim 10$ guarantees a realistic degree of smoothness. Consistent with this, the spacing between points on the profile need not be less than about $\Delta x = L_p/10 = \pi/5$. We chose $\Delta x = \pi/10$ in the present simulations. Our interest here is in the spacing of the fold hinges. We do not expect a long segment of layer to survive the folding process without developing fold hinges. Thus, we can set the restriction $k_n \gtrsim 0.2$, eliminating wavelengths larger than 5 L_p. In the simulations we summed components with wavenumbers between 0.1 and 10 unless the amplitudes fell to very small values in this range. In this case, we truncated the spectra at wavenumbers such that the minimum amplitude was about 0.01 to 0.05.

Fold arc length.—The fold hinges in the low limb-dip fold train lie at the local minima and maxima along the fold train profile. In the large-amplitude fold train the distance between these are preserved as the arc distances between successive hinges.

The fold arc-length L is here defined as *twice* the distance (measured in units of layer thickness) between successive fold hinges (see Hudleston, 1973a,b). In a population of folds, L will have a frequency distribution $f(L)$. We might anticipate that the distribution of L will have a single well-defined maximum, and measured distributions (Sherwin and Chapple, 1968; Hudleston, 1973a) bear this out. A measure of the regularity of folding is given by the dispersion of $f(L)$,

$$\delta = \sigma/\bar{L}, \tag{6}$$

where σ is the standard deviation of $f(L)$, and $\bar{L}$ is the mean value of L. Sherwin and Chapple (1968) have measured *average fold arc-lengths* for short segments of fold trains. This quantity is computed by dividing the total arc-length between the first and last hinges in the segment by the number of folds, or, if N is the number of hinges, by (N−1)/2. Each value obtained was incorporated into a frequency distribution weighted by the number of folds in the segment. The frequency distribution of this quantity will have a much smaller dispersion than the corresponding frequency distribution of L, but it will have the same mean. Hudleston (1973a,b) gives several frequency distributions of L.

Examples of simulated and real fold train segments.—Examples of portions of simulated fold train segments are shown in figure 2. Since these are intended to represent low amplitude folds with limb dips of 10° to 15°, the vertical scale is exaggerated by a factor of at least 5. The vertical exaggeration brings out the positions of the hinges. For comparison, large amplitude natural folds selected from those studied by Sherwin and Chapple (1968) are shown in figure 1. Ignoring differences in fold morphology one can visually roughly match the natural fold train segments and the simulated folds in terms of the degree of regularity. The natural fold segments would appear to have a degree of regularity greater than that of the simulation for $\beta = 1.5$ but less than that for the simulation $\beta = 0.58$.

In figure 2, some less prominent extrema are present. Should we select only prominent extrema as fold hinges? In figure 1, features corresponding to poorly developed hinges are likewise present. Since such features are present in the natural folds, we might conclude that the less prominent extrema are preserved as well in the finite-amplitude folding process. We therefore designated all extrema as fold hinges.

Frequency distributions of L.—Values of L were determined from the simulations by taking the differences in the x-coordinates of successive extrema. Their locations were determined more precisely than the increment Δx by interpolation. The distributions of L are given in the form of histograms with intervals of width 0.1 centered at values 0.05 L_p, 0.15 L_p, 0.25 L_p, et cetera.

Figure 3 gives some indication of the variation among histograms obtained for each of 10 simulations of length 50 L_p. The shaded bars are bounded vertically by the greatest and least number of values of L falling in each interval. No individual histograms are shown here: the upper or lower envelopes are not themselves histograms. Figure 4 shows the cumu-

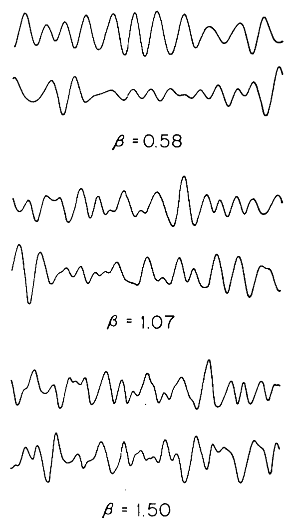

Fig. 2. Simulated fold-train segments for different amplitude spectrum bandwidths, β.

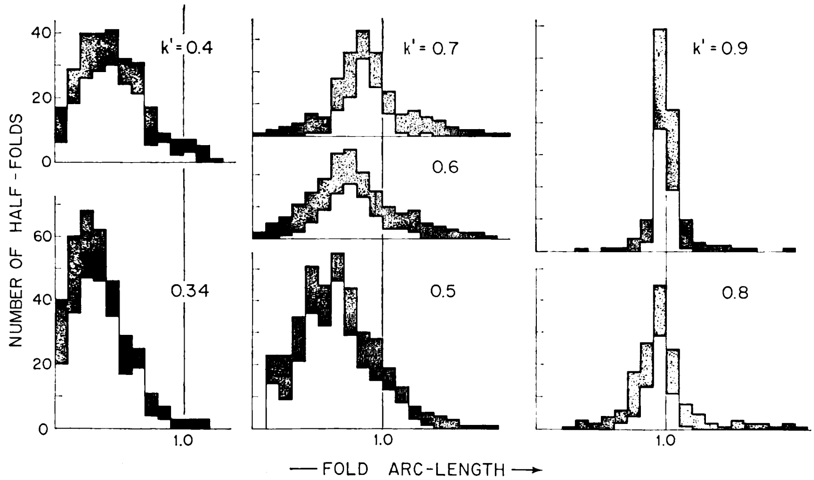

Fig. 3. Ranges of frequency distribution in fold arc-length measured from simulated fold train profiles.

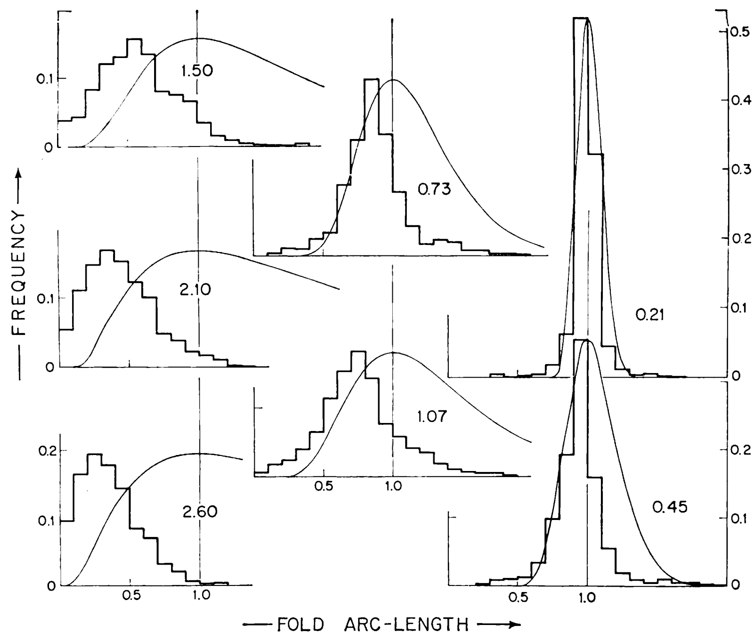

Fig. 4. Comparison of frequency distributions of fold arc length and amplitude spectra used to synthesize fold train profiles. The number labelling each pair is the relative bandwidth of the amplitude spectrum.

lative histograms for 10 and sometimes more simulations of length 50 L_p, recast in terms of frequency. The amplitude spectra, normalized so that the maxima value is numerically equal to the maximum frequency, are superposed, using the same numerical scales for L and *L*. The light vertical lines are at the values L_p.

It can be seen immediately from figure 4 that the most frequent value of *L* is always smaller than L_p and that the difference increases as the bandwidth of the spectrum increases.

Empirical relationships between arc-length frequency distribution and amplitude spectra.—The most frequent value of *L* is relatively poorly determined by the data. A better value, more precisely located than the histogram interval, might be computed by a smoothing or interpolation procedure. In any case, this value has no particular significance. Thus, we prefer to consider the better determined global property, $\bar{L}$.

Values of the ratio $\bar{L}/L_p$ and δ determined in the simulations are plotted against each other in figure 5. Each solid circle represents a pair of values for a single simulation of length 50 L_p. The scatter indicates the reliability of an estimate of these parameters from a sample of this size, which might be typical of the size of a set of field observations dictated by the availability of material. [Only two of Sherwin and Chapple's (1968) fold populations are larger than this.] The open circles are averages for five or, in most cases, ten such simulations. The smooth curve shown is well determined by these data; the curve is a free-hand fit.

Thus, if the present simulation realistically models natural fold trains, the value of dispersion δ may be used to assign a value to ratio $\bar{L}/L_p$. Likewise, the plot of relative bandwidth of the spectrum versus the dispersion (fig. 6) may be used to determine the relative bandwidth β of the low limb-dip amplitude spectrum.

$\bar{L}$ as an estimate for the wavelength of the component with maximum limb-dip.—Amplitude per se does not, in fact, play a very signifi-

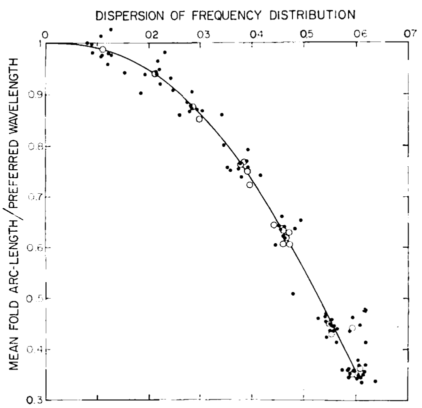

Fig. 5. Ratio of mean fold arc length to preferred wavelength $\overline{L}/L_p$ versus the dispersion of the frequency distribution, δ.

cant role in describing the layer shape insofar as the delineation of folds is concerned. To see this, imagine that the shape is formed by a superposition of only two sinusoidal components, one with a wavelength much longer than the other, but both with the same amplitude. What we will see is a train of folds with arc-lengths approximately equal to the smaller wavelength. The longer wavelength form will not contribute significantly to the spacing of the maxima in curvature and will contribute merely a gentle undulation to the fold train.

This suggests that limb-dip, rather than amplitude, is the more important property of a component in the profile shape. The comparison of $\bar{L}$ with L_p may therefore obscure a simpler relation. The spectrum of limb-dip θ, or alternatively of the tangent of the limb-dip, is obtained by multiplying the amplitude times the wavenumber

$$\tan \theta = \mathrm{kA(k)}. \tag{7}$$

The maximum of this spectrum must always lie at a larger value of k than the maximum of the amplitude spectrum or at a smaller value of the wavelength. Let L_θ be the wavelength of the component with the maximum limb-dip. The values of L_θ for the spectra used in the synthesis are compared with the corresponding values of $\bar{L}$ in figure 7. The approximation

$$L_\theta \cong \bar{L} \tag{8}$$

fits the data reasonably well, although $\bar{L}$ is always somewhat smaller than L_θ. On the basis of the present work, it is not possible to say whether some or all of the deviation from (8) can be ascribed to the simulation procedure. It would be safer to treat (8) as a reasonably good empirical relation for the interpretation of frequency distribution data from na-

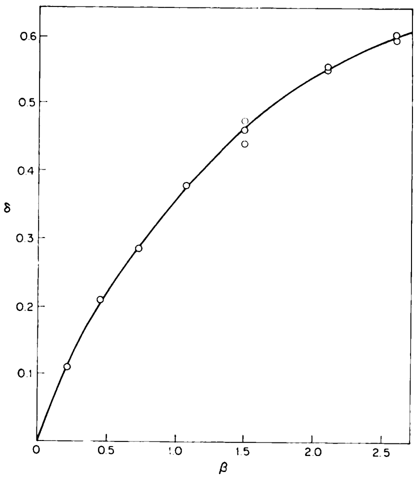

Fig. 6. Dispersion of the frequency distribution of fold arc length versus the relative bandwidth of the amplitude spectrum, β.

tural fold populations rather than as a statement of some underlying necessary relation between these quantities.

DISCUSSION

Initial amplitude spectrum.—The interpretation of fold arc-length data from natural fold populations involves two steps. We have shown how the frequency distribution of arc lengths can be related to the low limb-dip amplitude spectrum. The amplitude spectrum, in turn, is related to theory through the amplification spectrum, but the relation depends upon the initial amplitude spectrum. The initial amplitude spectrum can be determined only by measurement of surfaces of unfolded layers. We can, however, make a fair guess as to its probable form.

When we choose an initial amplitude spectrum, we also fix the variation of the initial limb-dip of a wavelength component. The choice of an uniform initial amplitude spectrum $A(k,0) = A_0$ has the merit of simplicity, but it leads to an initial limb-dip that increases with decreasing wavelength. An equally simple choice for the initial amplitude spectrum is one for which the initial limb-dip is uniform. From (7), this is

$$A(k,0) = \tan\theta_0/k, \tag{9}$$

where θ_0 is the initial limb-dip. The amplitude increases with increasing wavelength. Nine is called a "white roughness" spectrum (Kamb, 1970). The roughness at a given wavelength is measured by the slope, tan θ, which in this case in independent of wavelength. This means that at whatever length scale — that is, "magnification" — we look at the surface, its appearance will be the same. A surface corresponding to a flat amplitude spectrum looks rougher as the magnification is increased.

Some evidence exists that favors the choice of a white roughness spectrum, in that the spectra of a variety of three-dimensional surfaces

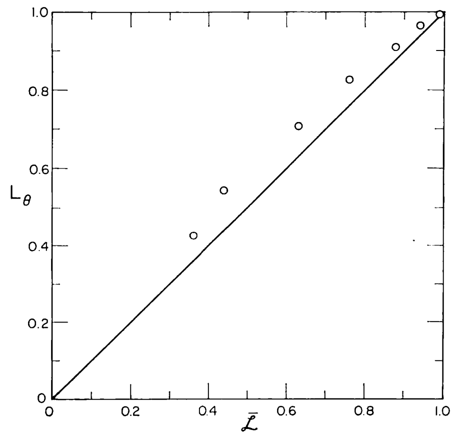

Fig. 7. Comparison of the mean fold arc length ($\bar{L}$) and the wavelength (L_θ) of the component with maximum limb dip.

have approximately this form. These surfaces include: terrain at Mare Cogitum, the Bonito lava flow, Arizona, a grass airport runway, and a vehicle test course, all cited in Jaeger and Schuring (1966); profiles through abyssal hills topography and the Earth's topography (Bell, 1975); and glacially abraded surfaces (Bernard Hallet, personal commun., 1976).

Another argument in favor of the choice of a white roughness spectrum is given in Kamb (1970). In the absence of any data, we wish to choose the spectrum that will introduce the least bias into the results. If the limb-dip of the components is the significant property, then we should choose a white roughness spectrum rather than a spectrum corresponding to uniform amplitude. Both spectra are equally simple in form, of course.

$\bar{L}$ as an estimate for the wavelength of the most-amplified component.—If the initial amplitude spectrum corresponds to uniform limb-dip, the spectrum of tan θ is

$$\tan \theta = \mathrm{k\ A = k\ A(k,0)}\mathbf{A}\mathrm{(k) = k(\tan\theta_0/k)A} = \tan\theta_0\mathbf{A}, \tag{11}$$

where $\mathbf{A}$ is the amplification spectrum. The wavelength for which the limb-dip is a maximum therefore is the same as that for which the amplification is a maximum, L_{max},

$$L_\theta = L_{max}, \tag{12}$$

and from (8),

$$\bar{L} \cong L_{max}. \tag{13}$$

Thus, relation (13), upon which all previous interpretations of fold arc length have been based, is a valid approximation provided the initial amplitude spectrum corresponds to uniform limb-dip. In contrast, if the initial amplitude spectrum corresponds to uniform amplitude, the maximum of the amplitude spectrum will coincide with that of the amplification spectrum, or

$$L_p = L_{max}. \tag{14}$$

The relationship between L_{max} and $\bar{L}$ is then that given in figure 5. $\bar{L}$ will generally be less than L_{max} by 20 to 30 percent.

A relation between dispersion and maximum amplification.—The dispersion of the frequency distribution of fold arc-length δ can be used to estimate the relative bandwidth of amplitude spectrum β. If the initial amplitude spectrum corresponds to uniform initial limb-dip, we have

$$\mathbf{A}\mathrm{(k)} \sim \mathrm{k\ A(k)}. \tag{15}$$

This relation suggests that we can estimate in turn the relative bandwidth of the amplification spectrum from that of the amplitude spectrum. Theory then supplies a relationship between the relative bandwidth of the amplification spectrum and the maximum amplification (Biot, 1961). As a final result, we should be able to estimate the maximum amplification from the dispersion.

Here we use the analytical form of amplitude spectrum (1) to find the relative bandwidth of amplification spectrum (15). The values of wavenumbers k* and k** at which **A** is equal to one-half its maximum value are given by

$$ln\ k^* = [1-(ln\ k')/(ln\ 0.5)]ln\ k',\ ln\ k^{**} = [-1-(ln\ k')/\ (ln\ 0.5)]\ ln\ k' \quad (16)$$

The amplification spectrum is a maximum at k_p^*, where

$$ln\ k_p^* = -(1/2)\ (ln\ k')/(ln\ 0.5) \quad (17)$$

the relative bandwidth of the amplification spectrum is then

$$\beta^* = (k^{**}-k^*)/k_p^* \quad (18)$$

The relation between β^* and β established by (4) and (17) is used with relation $\delta = \delta(\beta)$ (fig. 6), to establish the relation between δ and β^* shown in figure 8.

In the approximate analysis given by Biot (1961), the maximum amplification is uniquely determined by the relative bandwidth of the amplification spectrum, independent of the rheological parameters. Use of exact results (Fletcher, 1974) shows a significant dependence on rheological parameters (fig. 9). A major part of this dependence is due to the fact that the exact result includes the effect of the non-selective kinematic amplification, while the approximation does not. As a consequence, higher total amplification is required to obtain the selective amplification that leads to bandwidth reduction. Also, the curves of amplification versus bandwidth are shifted upward by an amount that depends on the ratio of selective amplification to kinematic amplification for given rheological parameters. A consequence of this is that the minimum relative bandwidth attained when the folding instability is weak can be quite large.

Hudleston (1973b) reports a set of data for ptygmatic folds for which the mean is $\bar{L} = 3.7$, and the dispersion is $\delta = 0.40$. From the empirical relations, this implies a value $\beta = 1.21$ for the amplitude spectrum and a value $\beta^* = 1.54$ for the amplification spectrum. The Biot approximation yields a maximum amplification of 2. If the layer behaved like a linear

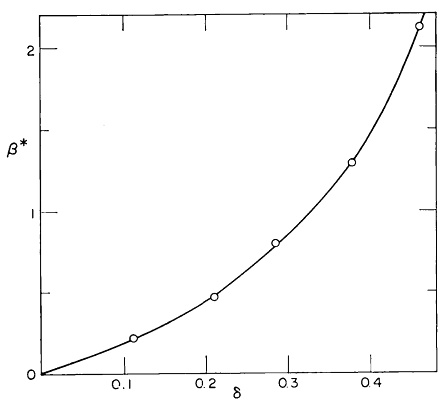

Fig. 8. Correlation of β^* with δ.

viscous fluid, the maximum amplification would range from about 7 for a viscosity ratio of 1/100 to about 50 for a viscosity ratio of 0.08. If the layer behaved like a power-law fluid with exponent n = 3, the maximum amplification would be about 7. Hudleston (1973) suggests amplification values of between 8 and 30.

For the largest fold population studied by Sherwin and Chapple (1968), the mean fold arc length is $\bar{L} = 6.1$, and the dispersion is $\delta' = 0.33$. We write δ' for the dispersion here because Sherwin and Chapple consider a different fold arc length, the mean value over a fold-train segment, which enters their frequency distribution weighted by the number of folds in the segment. The dispersion of this quantity should be much smaller than the dispersion for the fold arc length considered here. An interpretation of δ' in terms of maximum amplification cannot be made on the basis of available information. The dispersion, δ', obtained, however, is surprisingly large, since we would expect $\delta \gtrsim 2\delta'$ at least. The probable reason is that the frequency distributions obtained in the present numerical simulations are free of any contribution to the dispersion from precision and reproducibility of measurement, which in the observation of natural folds includes both measurements of fold arc length and layer thickness. Without the evaluation of this contribution to the dispersion estimates of amplification, use of the present results will yield only minimum values.

ACKNOWLEDGMENTS

We thank William M. Chapple and Arvid M. Johnson for helpful reviews. We thank Perfecto Mari for preparing the final drafts of the figures and Marie Phillips for typing the manuscript.

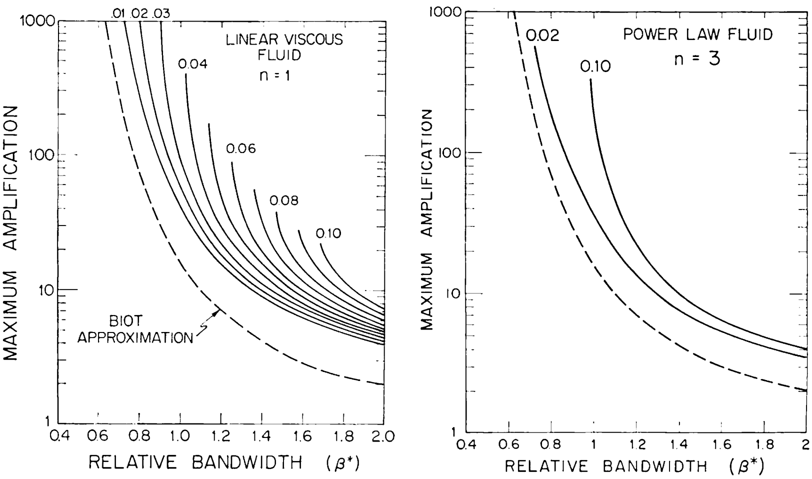

A. B.

Fig. 9. Maximum amplification versus relative bandwidth of amplification spectrum for: (A) Linear viscous layer and (B) layer with power-law exponent 3. The value labelling separate curves is the ratio of the effective viscosity of the medium to that of the layer.

References

Bell, T. H., Jr., 1975, Statistical features of sea-floor topography: Deep-Sea Research, v. 22, p. 883-892.

Biot, M. A., 1961, Theory of folding of stratified viscoelastic media and its implications in tectonics and orogenesis: Geol. Soc. America Bull., v. 72, p. 1595-1620.

Biot, M. A., Ode, H., and Roever, W. L., 1961, Experimental verification of the theory of folding of stratified viscoelastic media: Geol. Soc. America Bull., v. 72, p. 1621-1632.

Cobbold, P. R., 1975, Fold propagation in single embedded layers: Tectonophysics, v. 27, p. 33-351.

Currie, J. B., Patnode, H. W., Trump, R. P., 1962, Development of folds in sedimentary strata: Geol. Soc. America Bull., v. 73, p. 655-674.

Fletcher, R. C., 1974, Wavelength selection in the folding of a single layer with power-law rheology: Am. Jour. Sci., v. 274, p. 1029-1043.

Hudleston, P. J., 1973a, An analysis of single-layer folds developed experimentally in viscous media: Tectonophysics, v. 16, p. 189-214.

———— 1973b, The analysis and interpretation of minor folds developed in the Moine rocks of Monar, Scotland: Tectonophysics, v. 17, p. 89-132.

Jaeger, R. M., and Schuring, D. J., 1966, Spectrum analysis of terrain of Mare Cognitum: Jour. Geophys. Research, v. 71, p. 2023-2028.

Kamb, B., 1970, Sliding motion of glaciers: theory and observation: Rev. Geophysics Space Physics, v. 8, p. 673-728.

Sherwin, J., and Chapple, W. M., 1968, Wavelengths of single layer folds: a comparison between theory and observation: Am. Jour. Sci., v. 266, p. 167-179.